Food Chemistry: X 25 (2025) 102205

Contents lists available at ScienceDirect

Food Chemistry: X

journal homepage: www.sciencedirect.com/journal/food-chemistry-x

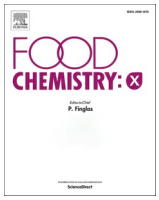

# Development of a novelly selective HPLC-chemiluminescence method by targeting degradation intermediates of nitroimidazoles and its application in animal food products

Mengdie Cai, Xinyu Wang, Kun Lu, Bixiao Zhou, Lijun Wei *, Xianglei Cheng *

*Jiangxi Province Key Laboratory of Preventive Medicine, School of Public Health, Nanchang University, Nanchang 330006, China.*

ARTICLE INFO

*Keywords:*
Nitroimidazoles
Mechanism
HPLC-Chemiluminescence detection
UV photolysis

ABSTRACT

Residues of nitro-containing drugs in food and the environment have aroused social concern because of their excessive use for the treatment of human and animal diseases. The disadvantages of complex and time-consuming pretreatments in existing methods make it imperative to develop novel methods. Herein, with the aid of recognition probe MCLA, an excellent selective method for the detection of nitroimidazoles (NDZs) was developed based on high-performance liquid chromatography combined with ultraviolet (UV) degradation and chemiluminescence (HPLC-UV-CL). The study proposed an innovative process for the formation of $SO_4^{\bullet-}$, •OH, and •NO via advanced oxidation processes of NDZs. Six studied NDZs achieved baseline separation within 24 min with detection limits as low as 3 ng/mL ($S/N = 3$). The proposed method is efficient, cost-effective, and does not require complicated purification steps. This study presents a unique approach for the detection of nitro-containing contaminants and provides new insights into monitoring advanced oxidation processes.

## 1. Introduction

Economic development has increased the average healthy life expectancy and the demand for medicines (Jaunay et al., 2023). Concurrently, a large number of drugs have been developed for diseases treatment of animals and meat preservation (Ludwiczak et al., 2024). The nitro group is an important functional moiety in pharmaceutical chemistry, characterized by its strong electron-accepting capacity, which can create localized electron-deficient sites within the molecule.

Nitro-containing drugs can interact with bionucleophilic entities such as proteins, amino acids, nucleic acids and enzymes (Nepali et al., 2019). Consequently, nitro groups are commonly found in various anti-tumor agents, antibiotics, anti-tuberculosis medications, anti-parasitic drugs, insecticides, and herbicides (Dziduch et al., 2024). The use of nitro-containing drugs, including gastric medications such as ranitidine (Kim et al., 2024), antimicrobial agents such as metronidazole (Walsh et al., 2024), and antibiotics such as nitrofurantoin (Hussein et al., 2024), is common in clinical practice. Currently, these drugs are also widely used to treat various diseases in animals. Various pharmaceuticals may persist in the body or be released into the environment during manufacturing, use, and disposal (Rairat et al., 2024), which leads to a series of health risks and poses a threat to the global environment and human health (Nordin et al., 2024; Wilkinson et al., 2022). Furthermore, these compounds are frequently associated with severe adverse reactions and toxicities, including carcinogenicity, hepatotoxicity, and mutagenicity (Wang et al., 2023). Therefore, monitoring nitro-containing drug residues is essential to ensure the safety of meat-based foods and safeguard human health (Shen et al., 2024; Yang et al., 2024).

Many methods for detecting and analyzing nitro-containing drug residues have been reported until now, for example, high performance liquid chromatography tandem mass spectrometry (HPLC-MS/MS) (Guo et al., 2017), electrochemical analysis (ECL) (Liu et al., 2021), enzyme-linked immunosorbent assays (ELISA) (Wang et al., 2011), and chemiluminescence (CL) (Chen et al., 2017). Among them, HPLC-MS/MS has gradually become one of the most commonly used methods (Melekhin et al., 2024). However, purification procedures such as solid-phase extraction (SPE) are inevitable when using HPLC-MS/MS, resulting in time consumption, complex pretreatment and high cost (Sasano et al., 2024). In order to address the challenges of global warming and reduce carbon emissions, the exploration of simpler, faster, safer, and more environmentally friendly detection methods is of importance (Gökmen, 2023; Jin et al., 2022). CL techniques have become popular in health inspection and drug analysis (Yu et al., 2024), and are active in the

* Corresponding authors at: School of Public Health, Nanchang University, 461 Bayi Road, Nanchang, 330006, PR China.
*E-mail addresses:* weilj7681@163.com (L. Wei), chengxlsd@163.com (X. Cheng).

https://doi.org/10.1016/j.fochx.2025.102205
Received 25 November 2024; Received in revised form 8 January 2025; Accepted 19 January 2025
Available online 21 January 2025

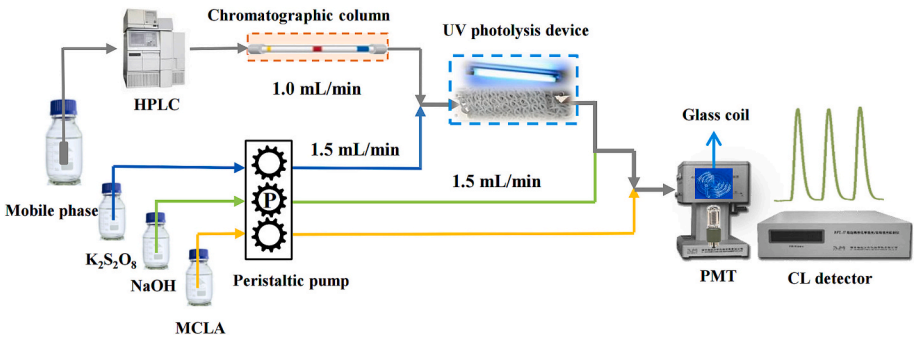


**Fig. 1.** Schematic diagram of the HPLC-UV-CL detection system.

multidisciplinary fields of chemistry, food, environment, life science, medicine, and materials (Cai et al., 2022; Shishavan & Amjadi, 2021). The combination of HPLC and CL (HPLC-CL) is helpful to solve the problem of matrix interference with the advantages of high sensitivity, high efficiency, and good selectivity (Wei, Cai, et al., 2024; Wei, Gan, et al., 2024).

Our previous studies (Ding et al., 2023) have demonstrated that substances containing N-$NO_2$ structure would produce nitrogen oxygen free radicals (·NO) after ultraviolet (UV) irradiation. Another interesting phenomenon was observed: NDZs reacted with 2-methyl-6-(4-methoxyphenyl) 3,7 dihydroimidazo[1,2-a]-pyrazin-3-one (MCLA) to produce a strong CL after UV photolysis using $K_2S_2O_8$ as the photolysis accelerator, and the CL intensity was positively correlated with concentration. Therefore, a new HPLC-UV-CL method was developed in order to detect the NDZs. By optimizing the HPLC and CL conditions, we applied this method for to monitor NDZs residues in chicken gizzards, chicken breast, lean meat, pork liver, and pork kidneys, with the detection limit as low as ng/mL. Additionally, we conducted in-depth studies of the reaction mechanism using fluorescence (FL) spectroscopy, CL spectroscopy, free-radical quenching experiments, and electron paramagnetic resonance techniques (EPR). This study provides a novel approach for the detection of nitro-containing drugs.

## 2. Materials and methods

### 2.1. Materials and reagents

Unless otherwise specified, all the reagents were used directly without further purification. Acetonitrile (ACN) and methanol (MeOH) were purchased from Merck group (Darmstadt, Germany). Formic acid (FA, HPLC grade) was purchased from Shanghai Aladdin Biochemical Technology Co., Ltd. (Shanghai, China). MCLA was acquired from TCI (Shanghai) Development Co., Ltd. (Shanghai, China), and potassium persulfate ($K_2S_2O_8$) was purchased from Tianjin Kaitong Chemical Reagent Co., Ltd. (Tianjin, China). For the six NDZs, metronidazole (MNZ) and dimetridazole (DMZ) were purchased from Beijing Innochem Technology Co., Ltd. (Beijing, China), ronidazole (RNZ) was purchased from Merck group (Darmstadt, Germany), tinidazole (TNZ) and secnidazole (SNZ) were acquired from TCI (Shanghai) Development Co., Ltd. (Shanghai, China), and ornidazole (ONZ) was purchased from Shanghai Macklin Biochemical Technology Co., Ltd. (Shanghai, China). The standard product was dissolved in methanol and prepared into 0.5 mg/mL reserve liquids that were stored at −4 °C.

The MCX solid phase extraction column utilized in this study was purchased from Waters Technologies (Milford, MA, USA). The required columns included the Dikma Diamonsil Plus C18-A (250 × 4.6 mm, 5 μm) (Beijing, China), Waters Xbridge BEH C18 (150 × 4.6 mm, 3.5 μm) (Milford, USA), and Waters SunFire C18 (250 × 4.6 mm, 5 μm) (Milford, USA).

### 2.2. Apparatus

The HPLC-UV-CL system consists of three main components: HPLC, UV photolysis, and CL detection. The HPLC system consisted of a Waters 2695 HPLC system (Waters, Milford, MA, USA) and thermostat column compartment. The UV photolysis device was purchased from Aura Industries Co., Ltd. (New York, NY, USA), and the wavelength of the UV lamp was 254 nm. The CL detection system was composed of a BT100-1F peristaltic pump (Baoding Longer Precision Pump, China), IFFS-A CL detector equipped with a glass coil, and RFL-I data analyzer (Xi'an Remex Analyze Instrument, China). A personal computer was used to obtain the experimental data. FL spectra were obtained using a FL spectrophotometer (F-320, Tianjin Gangdong Technology Co., Ltd., China), and CL spectra were measured using a FL spectrophotometer after blocking the xenon lamp emission window.

### 2.3. Condition of HPLC-UV-CL

A schematic representation of the HPLC-UV-CL detection system is shown in Fig. 1. All components were connected to polytetrafluoroethylene or peek tubes (0.8 mm id). Six NDZs were separated on a Waters SunFire C18 column using $H_2O$/ACN/1 % FA as the mobile phase at 25 °C. The injected volume was 100 μL. $K_2S_2O_8$, NaOH, and MCLA were transported using a peristaltic pump. $K_2S_2O_8$ was first mixed with the post-column products and allowed to flow through the UV photolysis device. Subsequently, the mixture was then mixed with NaOH and finally with MCLA in a flow cell to generate CL. The detection of the six NDZs was based on the change in CL intensity, $\Delta I = I_s - I_b$, where $I_s$ and $I_b$ were the CL intensities in the presence and absence of NDZs, respectively.

### 2.4. Sample preparation

Chicken gizzards, chicken brisket, lean meat, pork livers, and pork kidneys were purchased from a local market. After the chicken and pork were crushed, approximately 2 g of the sample was weighed into a 50 mL centrifuge tube, and the standard concentrations were set as follows: MNZ, DMZ, RNZ, and SNZ at 10 ng/mL, 20 ng/mL, 100 ng/mL; TNZ, and ONZ at 20 ng/mL, 40 ng/mL, and 200 ng/mL. The mixture was vortexed for 30 s, and 15 mL of ethyl acetate was added to the solution. The supernatant was then extracted by vortexing. The extraction steps were repeated twice, and the extraction solution was combined and dried with nitrogen at 25 °C. A total of 5 mL of 0.1 mol/L HCl solution was added to the residue, which was vortexed for 1 min to ensure complete dissolution. Subsequently, 5 mL of n-hexane was added, oscillated, centrifuged, and the n-hexane layer was discarded. Next, 5 mL of n-hexane was added to the lower layer for repeated defatting and the n-hexane layer was discarded. After the extraction process was completed, there was no need to use solid-phase extraction column for purification, and all samples were filtered through a 0.22 μm membrane before testing.

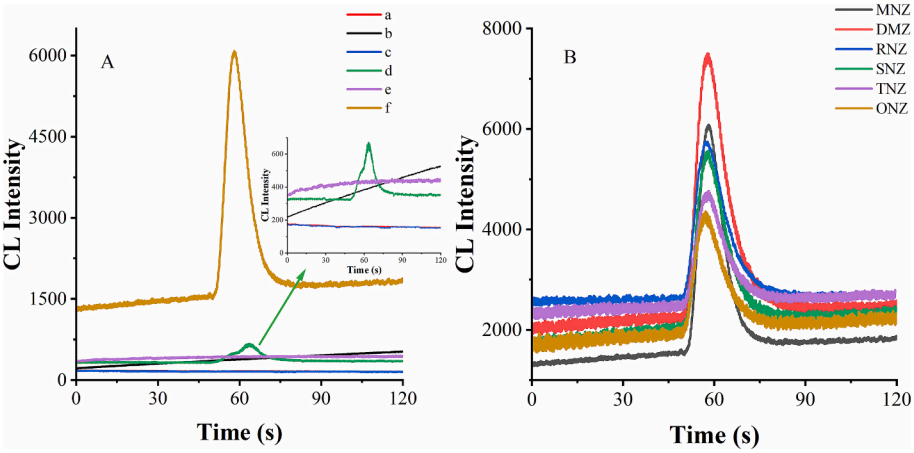


**Fig. 2.** Reaction kinetics curves. A: MCLA + $K_2S_2O_8$ - NO UV (a), MCLA + $K_2S_2O_8$ + MNZ - NO UV (b), MCLA + MNZ - NO UV (c), MCLA + $K_2S_2O_8$ – UV (d), MCLA + MNZ – UV (e), MCLA + $K_2S_2O_8$ + MNZ – UV (f); B: Kinetics curves of the six NDZs. Conditions: 0.5 μmol/L MCLA, 0.5 mmol/L $K_2S_2O_8$, 0.1 μg/mL NDZs.

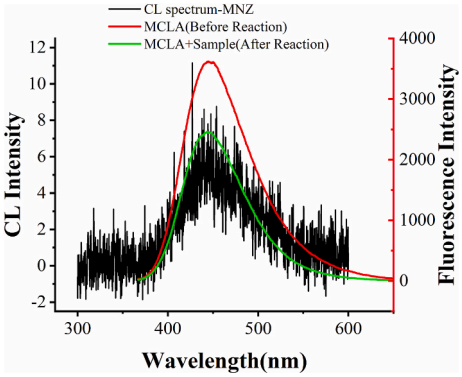


**Fig. 3.** CL spectra and FL spectra. Conditions: 0.2 μM MCLA, 5 mM $K_2S_2O_8$, CL flow rate: 1.8 mL/min, 0.2 μg/mL MNZ.

### 2.5. Statistical analysis

All experiments were performed in triplicate, and the results are presented as mean values. Data were analyzed using a paired sample *t*-test. $p < 0.05$ was considered significant.

## 3. Results and discussion

### 3.1. CL mechanism

The reaction kinetics curve of the CL system was obtained using an improved static injection method. The results are shown in Fig. 2: in the absence of UV irradiation, and with 5 mL of MCLA as the substrate, 150 μL of $K_2S_2O_8$ (Fig. 2A, line a) and 150 μL of MNZ (Fig. 2A, line c) were injected separately, and no CL was observed. When the substrate contained both MCLA and $K_2S_2O_8$, the baseline continued to rise. A total of 150 μL MNZ (Fig. 2A, line b) was then injected, and still no CL signal was observed. After the UV photolysis device was introduced, 150 μL of $K_2S_2O_8$ (Fig. 2A, line d) and 150 μL of MNZ (Fig. 2A, line e) was injected with 5 mL of MCLA as a substrate. The results demonstrated that the injection of $K_2S_2O_8$ produced a CL signal with an intensity of approximately 350, indicating that the free radicals generated by $K_2S_2O_8$ activated via UV irradiation could react with MCLA to produce a weak CL. In Fig. 2A, lines e and f represent the CL produced by the injection of 150 μL MNZ in the absence and presence of $K_2S_2O_8$, respectively. The results revealed that when there was no photolysis accelerator, almost no CL was present. After the mixed solution of NDZs/$K_2S_2O_8$ was degraded by UV light, it reacted with MCLA to produce a strong CL signal, reaching a maximum intensity at approximately 7.7 s, and indicating that there may be a new reaction in the system to produce a strong CL. Other NDZs exhibited similar CL phenomena (Fig. 2B).

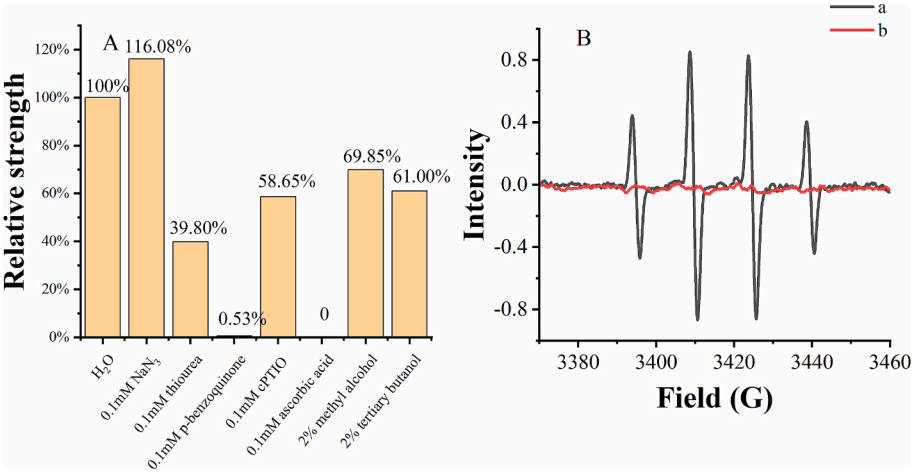


**Fig. 4.** Results of the free radical capture experiment (A) and electron paramagnetic resonance experiment (B). B-a: DMPO/•OH radical in $K_2S_2O_8$ /UV ; B-b: DMPO/•OH radical in $K_2S_2O_8$ + MNZ / UV.

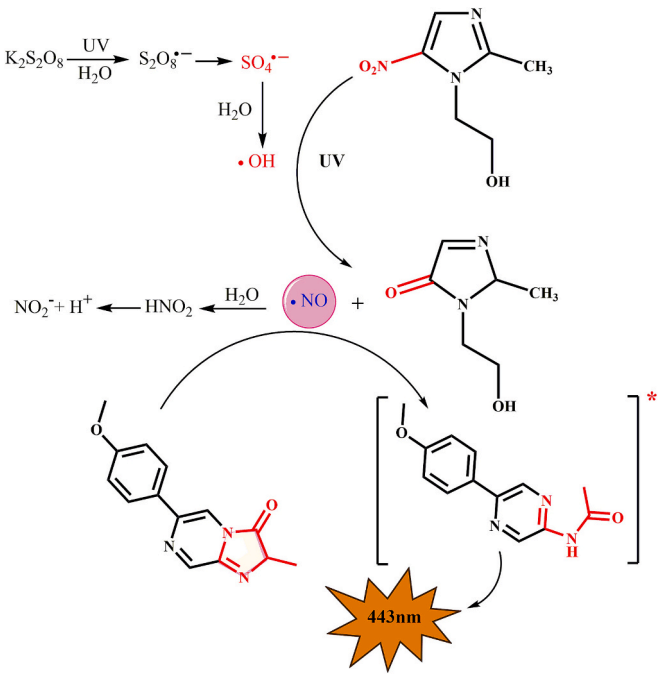


**Fig. 5.** Schematic diagram of the reaction mechanism of the NDZs / $K_2S_2O_8$ (UV) - MCLA system.

The FL and CL spectra of the system were measured to elucidate the mechanisms. The emission spectra of the MCLA before and after the reaction were obtained using a FL spectrophotometer. At the maximum excitation wavelength, the emission peaks before and after the reactions are located near 443 nm (Fig. 3). However, the intensity of the emission peak after the reaction was lower than that before the reaction, indicating that the structure of MCLA changed slightly after the reaction. An improved FL spectrophotometer was used to obtain CL spectra of the system. The wavelength of the CL spectrum was approximately 443 nm, which was consistent with the FL spectrum of MCLA after the reaction (Fig. 3), indicating that MCLA participated in the reaction and was the main contributor to the CL signal. Moreover, the wavelength of this CL system was 443 nm, which was different from the 460 nm generated by the reaction of $^1O_2$ or $O_2^-$ with MCLA (Zeng et al., 2017), indicating that $^1O_2$ and $O_2^-$ were not the key free radical.

Free-radical quenching experiments are a key step in exploring the types of free radicals involved in reaction (Zhang et al., 2019). Therefore, 0.1 mmol/L ascorbic acid, thiourea, sodium azide, and p-benzoquinone were used as free radical quenchers to explore the role of free radicals in the CL system (Fig. 4A). Owing to its strong reducibility, ascorbic acid could react with all free radicals (Brewer, 2011). In this experiment, ascorbic acid simultaneously quenched the CL of the samples and the background CL. These results indicated that free radicals played a key role in the reaction of $K_2S_2O_8$ with MCLA and in the luminescence effect of NDZs with MCLA. Furthermore, thiourea, sodium azide, and p-benzoquinone reacted directly with $K_2S_2O_8$ in this system. Therefore, they could not reflect the role of free radicals. The addition of cPTIO reduced CL intensity to 58.65 %, indicating that •NO may play a role in the system. Methanol and tert-butanol were used as trapping agents of •OH/$SO_4^{\bullet-}$ and •OH, respectively (Cai et al., 2022). When 2 % methanol and tert-butanol were added to the system, the CL signal decreased by approximately 30–40 %, indicating that •OH and $SO_4^{\bullet-}$ were likely to exist in the system.

Electron paramagnetic resonance (EPR) was employed in order to determine the type of free radicals. The compound 5, 5-dimethyl-1-pyrroline N-oxide (DMPO) is a commonly used •OH trapping agent that can capture •OH and produce a characteristic peak at 1:2:2:1 (Liu et al., 2024). Fig. 4B presents the results of free-radical detection using EPR. Curve (a) indicates the characteristic peak of 1:2:2:1 produced by •OH captured by DMPO. Curve (b) indicates the EPR results after the addition of the NDZs. The characteristic peaks of •OH disappeared, and no characteristic peaks of other free radicals were observed. This indicated that $K_2S_2O_8$ could produce •OH after UV irradiation and that •OH was completely reacted in the system.

The effect of dissolved oxygen on this system was also investigated. All reaction solutions, including $K_2S_2O_8$, MCLA, and the NDZs, were fed into $O_2$ and high-purity nitrogen for five minutes to compare the effects of dissolved oxygen. The baseline and CL signals of the NDZs/$K_2S_2O_8$(UV)-MCLA system exhibited little change after aeration and deaeration, indicating that the CL intensity of the NDZs/$K_2S_2O_8$ (UV)-MCLA system was independent of dissolved oxygen.

A possible reaction mechanism for the NDZs/$K_2S_2O_8$ (UV)-MCLA CL system was deduced based on the reaction kinetics curves, FL spectra, CL spectra, free-radical quenching experiments, and EPR experiments. As presented in Fig. 5, under the action of UV light, $K_2S_2O_8$ was first activated to produce $SO_4^{\bullet-}$, and $SO_4^{\bullet-}$ further reacted with water to produce •OH (Zeng et al., 2024), that then reacted with the nitro group of the NDZs to produce •NO and the corresponding carbonyl products via UV photolysis. •NO subsequently interacted with MCLA, making the MCLA transition to the excited state MCLA*. In the process of its return to the ground state, energy was released and CL signals were generated.

Previous research has demonstrated that the CL intensity is affected by many factors, including column type, mobile phase, column temperature, flow rate, and the type and concentration of the promoting media. These conditions were optimized in order to increase the S/N and reduce the detection limit. Under optimal conditions, the low detection limits, linear ranges, regression equations, correlation coefficients, and other indices were obtained.

### 3.2. Optimization of the HPLC conditions

Based on literature search, combined with the results of previous experiments, we compared the combined effects of various chromatographic columns with organic phases, acids, and buffer solutions (El-Maghrabey et al., 2021). We compared the separation results of the Diamonsil Plus C18-A, Xbridge BEH C18 and SunFire C18 columns and observed that the best separation results were obtained using the SunFire C18 column. MeOH, one of the most commonly used organic phases, was used in this study (Atapattu, 2023). The experimental results demonstrated that the CL signal was significantly inhibited even at a low concentration of MeOH, and this was related to the free-radical quenching effect of MeOH (Liu et al., 2019). The introduction of ACN also inhibited the CL signal in the sample. However, when a certain proportion of FA was introduced, the CL signal was significantly enhanced, and the baseline was stable. Based on this phenomenon, ACN and FA were selected as mobile phases for NDZs separation, and the elution procedure was optimized according to the separated substance. When the ratio of ACN was low, due to the strong interaction between the separated substance and C18 filler, the mobile phase elution ability was insufficient, resulting in serious peak broadening. This condition could not achieve separation of the six substances, and the analysis time was long. With increasing ACN ratio, the elution ability of the mobile phase was enhanced, the overall elution time of the separated substance was shortened, and the degree of separation increased. Concurrently, both the column temperature and column flow rate were optimized, and the column temperature exerted no obvious effect on the separation effect. Therefore 25 °C was chosen as the optimal temperature for separation. By optimizing the flow rate at 0.5–1.2 mL/min, we observed that although the separation of the six NDZs could be achieved when the flow rate was lower than 1.0 mL/min, the retention time was long, and a large amount of organic solvents was consumed. When the flow rate of the chromatographic pump continued to increase, TNZ could not be separated from the slope peak caused by the gradient change, and the S/N ratio decreased (Fig. S1). Therefore, when considering the separation

**Table 1**
Comparison of the performance on the detection of the NDZs with the different methods.

| Methods | NDZs | Pretreatment | ILOD (μg/kg) | MLOD (μg/kg) | Sample | References |
|---|---|---|---|---|---|---|
| HPLC-MS/MS | Seven NDZs | MISPE | 0.5–2.5 | 0.1–0.5 | Honey | (Guo et al., 2017) |
| HPLC-MS/MS | DMZ | SPE | 5.0 | 0.5 | Egg and chicken tissue | (Mo et al., 2024) |
| HPLC-UV | DMZ/RNZ/SNZ/MNZ/ONZ | SPE | 0. 2–0. 4, 4–10 5–7 | 0.02–0.04, 0.4–1.0 0.5–0.7 | Water, honey and chicken breast | (J. Wang et al., 2023) |
| Differential-pulse voltammetry technique (DPV) | RNZ | None | 107 | – | Bovine meat | (Diniz et al., 2020) |
| ECL | MNZ | None | 8.6 | – | Raw milk | (Liu et al., 2021) |
| HPLC-UV-CL | MNZ/DMZ/RNZ/SNZ/TNZ/ONZ | None | 3–6 | 0.5–1.0 | chicken gizzards, chicken breast, lean meat, pork liver, and pork kidneys | This work |

time and effect, we determined the optimal gradient elution procedure, as presented in Table S1.

### 3.3. Optimization of the CL conditions

The CL conditions of the system were optimized by considering the S/N ratio and baseline stability as dependent variables. Then we took six NDZs mixtures of 0.1 μg/mL MNZ, DMZ, RNZ, and SNZ and 0.2 μg/mL TNZ and ONZ as examples to observe the CL intensity under different conditions and construct the optimal reaction system.

Different mixing methods reflect different reaction orders, that exert an important influence on the CL intensity. Initially, we compared the effects of different mixing methods. The experimental results indicated that $K_2S_2O_8$, which functioned as a photolysis accelerator, could only generate a strong CL when subjected to UV photolysis in conjunction with NDZs. The introduction of an alkaline solution enhanced the CL signal; however, it must be added after UV photolysis in order to avoid a significant baseline drift. If the alkaline solution was pre-mixed with MCLA, the structure of MCLA would change, resulting in substantial background absorption. Consequently, when the NDZs were introduced into the system, no CL signals were observed. We determined that the best method was to first mix the post-column separation solution with $K_2S_2O_8$, which was then degraded under UV light and mixed with an alkaline solution. Finally, the mixture was mixed with MCLA in the coil, and the CL signals were recorded.

The flow rate of the peristaltic pump had a great influence on whether we could obtain the maximum S/N. When the flow rate was low, CL reaction did not occur in the detection cell. If the flow rate was too high, the solution would flow out before the CL reaction was completed. After studying the flow rate in the range of 1.0–2.2 mL/min, we observed that the maximum *S/N* ratio could be obtained when the flow rate was 1.5 mL/min, therefore, we determined that the optimal flow rate was 1.5 mL/min, as shown in Fig. S2.

The effects of different concentrations of NaOH, $Na_2CO_3$ and $NaHCO_3$ on the reaction system are compared, and the results are shown in Fig. S3. The introduction of an alkaline solution to neutralize FA in the mobile phase could increase the *S/N* ratio of the reaction system; however, if the concentration of the alkaline solution was too high, the CL intensity of MCLA would be strongly inhibited (Zeng et al., 2017). We determined that 0.01 mol/L NaOH was the best reaction solution.

MCLA, the only CL reagent used in this system, played an essential role in this study. The concentrations of MCLA ranging from 0.01 to 1.0 μmol/L were examined. The results were shown in Fig. S4 (A), which indicated that the S/N increased with increasing concentration in the range of 0.01–0.5 μmol/L. Then the CL intensity decreased when the concentration exceeded 0.5 μmol/L. This may be because the excess MCLA reacted with other substances to increase the noise, while the signal of the sample did not change significantly, and the S/N ratio decreased. Finally, 0.5 μmol/L MCLA was selected as the optimal reaction concentration.

The reaction between the NDZs degraded by UV irradiation and MCLA exhibited no CL signal and low efficiency, and the introduction of certain photolysis accelerators significantly improved the CL intensity. The effects of different oxidants, organic acids, and inorganic acids on this system were compared. The results revealed that $KIO_4$ had no significant effect on the CL of the system, whereas $KHSO_5$, acetic acid, HCl, $H_2SO_4$ and $H_2C_2O_4$ could enhance the CL of the system. Among these, $KHSO_5$ and $K_2S_2O_8$ yielded the best results. However, when $KHSO_5$ was introduced, it reacted directly with the MCLA to produce a strong background CL. $K_2S_2O_8$ provided a more stable baseline and signal; based on this, $K_2S_2O_8$ was introduced into the system as the best photolysis accelerator. The concentration of $K_2S_2O_8$ was optimized in the range of 0.5–8.0 mmol/L, and the effect is presented in Fig. S4 (B). When the concentration of $K_2S_2O_8$ was low, fewer free radicals were generated by $K_2S_2O_8$ after UV irradiation, and the photolysis-promoting effect on the NDZs was weak. With an increase in concentration, the promoting effect became increasingly evident. When the concentration reached 5.0 mmol/L, the promoting effect reached a maximum and the S/N ratio was the highest. As the concentration continued to increase, the *S/N* ratio decreased. Therefore, 5.0 mmol/L was selected as the optimal reaction concentration.

Finally, we optimized the detector voltage and compared the effects of voltage in the range of 300-600 V on the CL intensity. As shown in Fig. S5, as the voltage increased, the CL intensities of the six analytes gradually increased, and the noise increased. The maximum *S/N* was obtained at 400 V, and the continuous increase in the voltage exceeded the detection range of the instrument. Therefore, 400 V was chosen as the optimal voltage.

### 3.4. Method validation

This method was validated according to the 2002/657/EC Decision (European Commission, 2002). Under the aforementioned conditions, the standard chromatograms of the six NDZs were obtained using HPLC-UV-CL method (Fig. S6). The retention times for MNZ, DMZ, RNZ, SNZ, TNZ, and ONZ were 7.46, 9.49, 11.66, 13.20, 17.98, and 22.38 min, respectively, with a successful baseline separation within 24 min. Linearity, correlation coefficient (r), and limits of detection (LODs) were used to verify the accuracy of the method, and the relative standard deviation (RSD) was used to verify the precision of the method. The results are summarized in Table S2. The linear ranges of MNZ and SNZ were 20–1000 ng/mL and 20–2000 ng/mL, respectively. And the linear ranges of DMZ, RNZ, TNZ, ONZ were 10–1000 ng/mL. The correlation coefficients were all greater than 0.99 with LODs as low as 3 ng/mL ($S/N = 3$).

In Table 1, the proposed HPLC-UV-CL method is listed along with previously reported analytical techniques. In comparison, the detection limit of this method can reach a lower level. Moreover, for the pretreatment of complex substrates, this method does not require additional purification steps, and greatly reducs the sample processing time and reagent consumption. In addition, compared with mass spectrometry detectors, the use of CL detectors not only reducs costs, but also greatly

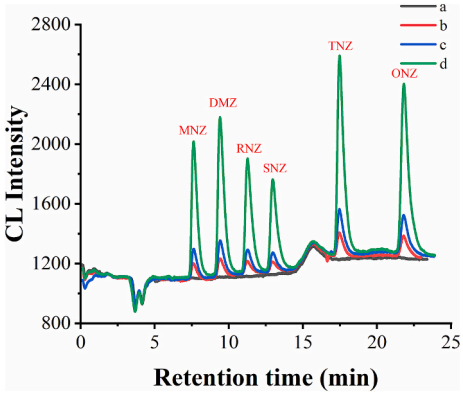


**Fig. 6.** Representative chromatogram of six NDZs in the samples of chicken gizzards unlabeled (a) and labeled (b, c, d) by HPLC-UV-CL. Conditions: 0.5 μM MCLA, 0.01 M NaOH, 5 mM $K_2S_2O_8$, CL flow rate: 1.5 mL/min, voltage: 400 V.

reducs carbon emissions.

The intraday RSDs were 3.44–5.97 % ($n = 6$) and the inter-day RSDs of the six analytes was 8.58–9.48 % over five days. Additionally, the sample recovery rate was in the range of 66.67–116.16 %. It was proven that the method had high sensitivity, a wide linear range, low detection limit, and good reproducibility, providing a new method for the detection of NDZs residues in chicken and pork.

### 3.5. Application

To evaluate the applicability of this method in real samples, NDZs were detected in chicken gizzards, chicken breast, lean meat, pork liver, and pork kidneys. The samples were extracted using different pretreatment methods and analyzed under optimal conditions. Each sample was repeatedly processed into three groups, and each group of samples was injected thrice in parallel. The spiked concentrations of MNZ, DMZ, RNZ, and SNZ were 10 ng/mL (Fig. 6, line b),20 ng/mL (Fig. 6, line c), 100 ng/mL (Fig. 6, line d), and the spiked concentrations of TNZ and ONZ were 20, 40, and 200 ng/mL. The CL intensity was used to reflect the content of each component, and the spiking recovery rates were calculated. The standard recovery rates for chicken and pork were listed in Table 2. NDZs residues were not detected in any of the tested samples. Fig. 6 presents the HPLC-UV-CL chromatographic separation of the six NDZs in chicken gizzards, demonstrating that the method exhibits good selectivity and separation. (See Table 2.)

A paired sample *t*-test was conducted on the sample detection results before and after purification with the solid-phase extraction column (Table S3) and the results revealed that the *p*-values for all six NDZs exceeded 0.05, indicating that there was no difference between the two pretreatment methods and that satisfactory recovery could be achieved without purification.

## 4. Conclusion

Based on the targeted recognition effect of MCLA on the NDZs UV photolysis intermediates, a new HPLC-UV-CL method was developed to detect six NDZs residues in chicken and pork. These findings revealed that the system exhibited high accuracy and selectivity for the detection of NDZs in chicken and pork and was essentially unaffected by matrix effects. This method was used to detect NDZs, and six samples were separated within 24 min, with a detection limit as low as 3 ng/mL (S/N = *3*). Furthermore, this method does not require complex purification steps during the pretreatment process, thereby improving the efficiency of the analysis and reducing detection costs. A mechanism study revealed the formation process of $SO_4^{\bullet-}$, •OH, and •NO and also revealed

**Table 2**
Determination of the NDZs in the different samples with the HPLC-UV-CL method.

| NDZs | Add(ng/mL) | Chicken breast | | Chicken gizzards | | Lean meat | | Pork liver | | Pig kidneys | |
|---|---|---|---|---|---|---|---|---|---|---|---|
| | | Found (ng/mL) | Recovery (%) | Found (ng/mL) | Recovery (%) | Found (ng/mL) | Recovery (%) | Found (ng/mL) | Recovery (%) | Found (ng/mL) | Recovery (%) |
| MNZ | 0 | ND | / | ND | / | ND | / | ND | / | ND | / |
| | 10 | 9.38 | 93.80 | 8.60 | 86.05 | 8.16 | 81.63 | 11.02 | 110.20 | 8.98 | 89.80 |
| | 20 | 18.15 | 90.76 | 16.97 | 84.87 | 19.80 | 99.00 | 17.00 | 85.00 | 20.40 | 102.00 |
| | 100 | 87.96 | 87.96 | 97.63 | 97.63 | 95.70 | 95.70 | 93.15 | 93.15 | 80.57 | 80.57 |
| DMZ | 0 | ND | / | ND | / | ND | / | ND | / | ND | / |
| | 10 | 10.42 | 104.20 | 9.51 | 95.10 | 6.67 | 66.67 | 10.53 | 105.26 | 8.25 | 82.46 |
| | 20 | 18.18 | 90.88 | 17.88 | 89.42 | 16.31 | 81.55 | 12.62 | 63.11 | 20.97 | 104.85 |
| | 100 | 82.55 | 82.55 | 90.63 | 90.63 | 94.09 | 94.09 | 95.51 | 95.51 | 111.82 | 111.82 |
| RNZ | 0 | ND | / | ND | / | ND | / | ND | / | ND | / |
| | 10 | 8.40 | 83.96 | 8.11 | 81.13 | 9.38 | 93.75 | 7.50 | 75.00 | 9.22 | 92.19 |
| | 20 | 17.86 | 89.29 | 16.33 | 81.63 | 20.15 | 100.74 | 13.82 | 69.12 | 19.41 | 97.06 |
| | 100 | 82.62 | 82.62 | 92.53 | 92.53 | 100.29 | 100.29 | 85.27 | 85.27 | 84.54 | 84.54 |
| SNZ | 0 | ND | / | ND | / | ND | / | ND | / | ND | / |
| | 10 | 9.08 | 90.80 | 8.05 | 80.46 | 9.77 | 97.67 | 11.16 | 111.63 | 10.23 | 102.33 |
| | 20 | 18.34 | 91.72 | 16.56 | 82.80 | 18.54 | 92.68 | 16.34 | 81.71 | 21.71 | 108.54 |
| | 100 | 83.23 | 83.23 | 92.92 | 92.92 | 104.62 | 104.62 | 106.59 | 106.59 | 87.69 | 87.69 |
| TNZ | 0 | ND | / | ND | / | ND | / | ND | / | ND | / |

**Table 2**
Determination of the NDZs in the different samples with the HPLC-UV-CL method (continued).

| | | | | | | | | | | | |
|---|---|---|---|---|---|---|---|---|---|---|---|
| | 20 | 15.24 | 76.22 | 16.54 | 82.70 | 19.22 | 96.08 | 22.55 | 112.75 | 22.55 | 112.75 |
| | 40 | 33.47 | 83.67 | 34.52 | 86.30 | 34.66 | 86.64 | 28.50 | 71.26 | 38.38 | 95.95 |
| | 200 | 166.53 | 83.27 | 180.54 | 90.27 | 203.98 | 101.99 | 210.86 | 105.43 | 181.36 | 90.68 |
| ONZ | 0 | ND | / | ND | / | ND | / | ND | / | ND | / |
| | 20 | 17.52 | 87.58 | 17.39 | 86.93 | 16.36 | 81.82 | 23.23 | 116.16 | 20.81 | 104.04 |
| | 40 | 33.19 | 82.99 | 34.86 | 87.15 | 39.32 | 98.31 | 35.25 | 88.14 | 43.84 | 109.60 |
| | 200 | 169.80 | 84.90 | 180.73 | 90.37 | 202.84 | 101.42 | 208.52 | 104.26 | 180.73 | 90.37 |

ND: Not detected.

the key roles of $SO_4^{\bullet-}$ and •OH in the degradation of NDZs. Additionally, this combined method provides a new idea for designing drug residue detection methods for food products.

## CRediT authorship contribution statement

**Mengdie Cai:** Writing – review & editing, Writing – original draft. **Xinyu Wang:** Methodology. **Kun Lu:** Methodology. **Bixiao Zhou:** Validation. **Lijun Wei:** Supervision, Methodology. **Xianglei Cheng:** Writing – review & editing, Funding acquisition, Conceptualization.

## Declaration of competing interest

The authors declare that they have no known competing financial interests or personal relationships that could have appeared to influence the work reported in this paper.

## Acknowledgements

The authors would like to thank for the financial supports from the National Natural Science Foundation of China (Nos. 82373631, 82173574 and 81960600) and Training Program of Innovation and Entrepreneurship for Undergraduates of Jiangxi Province (No. YC2023-B047).

## Appendix A. Supplementary data

Supplementary data to this article can be found online at https://doi.org/10.1016/j.fochx.2025.102205.

## Data availability

No data was used for the research described in the article.

## References

Atapattu, S. N. (2023). Selectivity comparison of acetonitrile-methanol-water ternary mobile phases on an octadecylsiloxane-bonded silica stationary phase. *Journal of Separation Science, 46*(23), Article e2300489. https://doi.org/10.1002/jssc.202300489

Brewer, M. S. (2011). Natural antioxidants: Sources, compounds, mechanisms of action, and potential applications. *Comprehensive Reviews in Food Science and Food Safety, 10*(4), 221–247. https://doi.org/10.1111/j.1541-4337.2011.00156.x

Cai, M., Gan, W., Ding, Z., Cai, H., Wei, L., & Cheng, X. (2022). Studies on reaction mechanisms and distinct chemiluminescence from cyanoimino neonicotinoids triggered by peroxymonosulfate in advanced oxidation processes. *Chinese Chemical Letters*. https://doi.org/10.1016/j.cclet.2022.05.068

Chen, J., Shu, J., Chen, J., Cao, Z., Xiao, A., & Yan, Z. (2017). Highly luminescent S,N co-doped carbon quantum dots-sensitized chemiluminescence on luminol-$H_2O_2$ system for the determination of ranitidine. *Luminescence, 32*(3), 277–284. https://doi.org/10.1002/bio.3173

Ding, Z., Cai, M., Gan, W., Yuan, P., Wei, L., & Cheng, X. (2023). Studies on a novel method for the determination of nitrosamines in food by HPLC-UV-FLD coupling with terbium-doped carbon dots. *Food Chemistry, 405*, Article 134894. https://doi.org/10.1016/j.foodchem.2022.134894

Diniz, J. A., Okumura, L. L., Aleixo, H., Gurgel, A., & Silva, A. F. S. (2020). A voltammetric screening method to determine ronidazole in bovine meat. *Journal of Environmental Science and Health, Part B, 55*(6), 583–591. https://doi.org/10.1080/03601234.2020.1745523

Dziduch, K., Janowska, S., Andrzejczuk, S., Strzyga-Łach, P., Struga, M., Feldo, M., … Wujec, M. (2024). Synthesis and biological evaluation of new compounds with nitroimidazole moiety. *Molecules, 29*(13), 3023. https://doi.org/10.3390/molecules29133023

El-Maghrabey, M., Suzuki, H., Kishikawa, N., & Kuroda, N. (2021). A sensitive chemiluminescence detection approach for determination of 2,4-dinitrophenylhydrazine derivatized aldehydes using online UV irradiation – Luminol CL reaction. Application to the HPLC analysis of aldehydes in oil samples. *Talanta, 233*, Article 122522. https://doi.org/10.1016/j.talanta.2021.122522

European Commission. (2002). Decision of 2022/657/EC of 12 august 2002 implementing council directive 96/23/EC concerning the performance of analytical methods and the interpretation of results. *Official Journal of the European Communities*, (221), 8–36. L.

Gökmen, V. (2023). Importance of food authentication and origin testing. *Food Chemistry: X, 18*. https://doi.org/10.1016/j.fochx.2023.100708

Guo, X.-C., Xia, Z.-Y., Wang, H.-H., Kang, W.-Y., Lin, L.-M., Cao, W.-Q., … Zhou, W.-H. (2017). Molecularly imprinted solid phase extraction method for simultaneous determination of seven nitroimidazoles from honey by HPLC-MS/MS. *Talanta, 166*, 101–108. https://doi.org/10.1016/j.talanta.2017.01.047

Hussein, M., Sun, Z. T., Hawkey, J., Allobawi, R., Judd, L. M., Carbone, V., … Velkov, T. (2024). High-level nitrofurantoin resistance in a clinical isolate of a comparative genomics and metabolomics analysis. *Msystems, 9*(1), 1–16. https://doi.org/10.1128/msystems.00972-23

Jaunay, E. L., Simpson, B. S., White, J. M., & Gerber, C. (2023). Using wastewater-based epidemiology to evaluate the relative scale of use of opioids. *Science of the Total Environment, 897*. https://doi.org/10.1016/j.scitotenv.2023.165148

Jin, Y., Dou, M., Zhuo, S., Li, Q., Wang, F., & Li, J. (2022). Advances in microfluidic analysis of residual antibiotics in food. *Food Control, 136*. https://doi.org/10.1016/j.foodcont.2022.108885

Kim, Y.-S., Park, Y., Kim, Y., Son, H.-E., Rhee, J., Pyun, C.-W., … Kim, H. (2024). Ameliorative effects of HT074-Inula and Paeonia extract mixture on acute reflux esophagitis in rats via Antioxidative activity. *Antioxidants, 13*(8), 891. https://doi.org/10.3390/antiox13080891

Liu, D., Giri, B. R., & Farooq, A. (2019). A shock tube kinetic study on the branching ratio of methanol + OH reaction. *Proceedings of the Combustion Institute, 37*(1), 153–162. https://doi.org/10.1016/j.proci.2018.05.179

Liu, G., Gao, H., Chen, J., Shao, C., & Wang, P.-L. (2021). Metronidazole determination in raw milk with a graphene aerogel-based electrochemiluminescent sensor and its effect on cell apoptosis. *Food Analytical Methods, 14*(7), 1415–1424. https://doi.org/10.1007/s12161-021-01982-w

Liu, J., Zhang, J., Weng, S., Xu, Z., Zhang, Y., Hou, T., & Zhu, W. (2024). A new catalyst derived from the sulfur-doped metal-organic framework for Fenton-like reaction. *Process Safety and Environment Protection, 191*, 1659–1671. https://doi.org/10.1016/j.psep.2024.09.082

Ludwiczak, A., Składanowska-Baryza, J., Cieślak, A., Stanisz, M., Skrzypczak, E., Sell-Kubiak, E., … Racewicz, P. (2024). Effect of prudent use of antimicrobials in the early phase of infection in pigs on the performance and meat quality of fattening pigs. *Meat Science, 212*, Article 109471. https://doi.org/10.1016/j.meatsci.2024.109471

Melekhin, A. O., Tolmacheva, V. V., Goncharov, N. O., Apyari, V. V., Parfenov, M. Y., Bulkatov, D. P., … Zolotov, Y. A. (2024). Rapid multi-residue LC-MS/MS determination of nitrofuran metabolites, nitroimidazoles, amphenicols, and quinolones in honey with ultrasonic-assisted derivatization – Magnetic solid-phase extraction. *Journal of Pharmaceutical and Biomedical Analysis, 237*. https://doi.org/10.1016/j.jpba.2023.115764

Mo, K., Wei, C., Bai, M., Long, X., Liu, X., & Ding, H. (2024). Elimination patterns of dimetridazole in egg of laying hens and tissues of broiler after oral administration. *Frontiers in Veterinary Science, 11*. https://doi.org/10.3389/fvets.2024.1451904

Nepali, K., Lee, H. Y., & Liou, J. P. (2019). Nitro-group-containing drugs. *Journal of Medical Chemistry, 62*(6), 2851–2893. https://doi.org/10.1021/acs.jmedchem.8b00147

Nordin, A. H., Yusoff, A. H., Husna, S. M. N., Noor, S. F. M., Norfarhana, A. S., Paiman, S. H., … Abdullah, N. (2024). Recent advances in nanocellulose-based adsorbent for sustainable removal of pharmaceutical contaminants from water bodies: A review. *International Journal of Biological Macromolecules, 280*. https://doi.org/10.1016/j.ijbiomac.2024.135799

Rairat, T., Keetanon, A., Phansawat, P., Chongprachavat, N., Pichitkul, P., Kitsanayanyong, L., … Chuchird, N. (2024). The presence of semicarbazide in crustaceans collected from natural habitats in Thailand. *Chemosphere, 347*, Article 140686. https://doi.org/10.1016/j.chemosphere.2023.140686

Sasano, R., Sekizawa, J., Saito, I., Harano, M., Katsumoto, K., Ito, R., … Akiyama, H. (2024). Simultaneous determination of glyphosate, glufosinate and their metabolites in soybeans using solid-phase analytical derivatization and LC-MS/MS determination. *Food Chemistry: X, 24*. https://doi.org/10.1016/j.fochx.2024.101806

Shen, H.-T., Pan, X.-D., & Han, J.-L. (2024). Comprehensive analysis and probabilistic health risk assessment of antimicrobial residues in farmed shrimp from Southeast China. *Journal of Food Composition and Analysis, 135*, Article 106598. https://doi.org/10.1016/j.jfca.2024.106598

Shishavan, Y. H., & Amjadi, M. (2021). A new enhanced chemiluminescence reaction based on polymer dots for the determination of metronidazole. *Spectrochimica Acta Part A-Molecular and Biomolecular Spectroscopy, 260*, Article 119992. https://doi.org/10.1016/j.saa.2021.119992

Walsh, L., Lavelle, A., O'Connor, P. M., Hill, C., & Ross, R. P. (2024). Comparison of fidaxomicin, thuricin CD, vancomycin and nisin highlights the narrow spectrum nature of thuricin CD. *Gut Microbes, 16*(1), Article 2342583. https://doi.org/10.1080/19490976.2024.2342583

Wang, J., Liu, J., Liu, W., Guo, Y., Wu, Q., Wang, Z., & Yan, H. (2023). Porphyrin-based hypercrosslinked polymers as sorbents for efficient extraction of nitroimidazoles from water, honey and chicken breast. *Journal of Chromatography A, 1702*. https://doi.org/10.1016/j.chroma.2023.464087

Wang, Y., He, F., Wan, Y., Meng, M., Xu, J., Zhang, Y., … Xi, R. (2011). Indirect competitive enzyme-linked immuno-sorbent assay (ELISA) for nitroimidazoles in food products. *Food Additives and Contaminants Part a-Chemistry Analysis Control Exposure & Risk Assessment, 28*(5), 619–626. https://doi.org/10.1080/19440049.2011.563366

Wei, L., Cai, M., Zhou, B., Yuan, P., Zhang, G., & Cheng, X. (2024). Novel Sulphur-selective method for simultaneous determination of thiram and asomate based on carbon dots and its application in fruits. *Food Chemistry: X, 24*. https://doi.org/10.1016/j.fochx.2024.101879

Wei, L., Gan, W., Cai, M., Cai, H., Zhang, G., & Cheng, X. (2024). Development of a novel HPLC-CDCL method utilizing nitrogen-doped carbon dots for sensitive and selective

detection of dithiocarbamate pesticides in tea. *Food Chemistry, 458*, Article 140237. https://doi.org/10.1016/j.foodchem.2024.140237

Wilkinson, J. L., Boxall, A. B. A., Kolpin, D. W., Leung, K. M. Y., Lai, R. W. S., Galban-Malagon, C., … Teta, C. (2022). Pharmaceutical pollution of the world's rivers. *Proceedings of the National Academy of Sciences of the United States of America, 119*(8), 1–10. https://doi.org/10.1073/pnas.2113947119

Yang, G., Zhang, J., Tang, Y., Kong, C., Li, S., Wang, S., … Chi, H. (2024). Development and validation of rapid screening of 192 veterinary drug residues in aquatic products using HPLC-HRMS coupled with QuEChERS. *Food Chemistry: X, 22*. https://doi.org/10.1016/j.fochx.2024.101504

Yu, F., Fan, B., Chai, Y., Liu, Y., Wang, J., Liao, Y., … Wang, Y. (2024). Antibiotic-$Fe_3O_4$ nanoparticles with highly efficient catalytic activity for enhanced chemiluminescence detection of tetracyclines residues in foods. *Food Chemistry: X, 22*. https://doi.org/10.1016/j.fochx.2024.101485

Zeng, W., Zhu, C., Liu, H., Liu, J., Cai, H., Cheng, X., & Wei, L. (2017). Ultrasensitive chemiluminescence of tetracyclines in the presence of MCLA. *Journal of Luminescence, 186*, 158–163. https://doi.org/10.1016/j.jlumin.2017.02.017

Zeng, Y., Qiu, H., Zeng, J., Gao, Y., Ding, Z., Xie, Z., & Wang, C. (2024). Degradation of beneficiation reagent ester-105 by light, heat, and microwave activated persulfate. *Water, Air, & Soil Pollution, 235*(2), 98. https://doi.org/10.1007/s11270-024-06906-y

Zhang, Y., Zhou, J., Chen, X., Wang, L., & Cai, W. (2019). Coupling of heterogeneous advanced oxidation processes and photocatalysis in efficient degradation of tetracycline hydrochloride by Fe-based MOFs: Synergistic effect and degradation pathway. *Chemical Engineering Journal, 369*, 745–757. https://doi.org/10.1016/j.cej.2019.03.108